Effect of the solar radiation of the Atacama desert in the design of a parabolic trough solar thermal power plant, using thermal oil in the solar field

Lorena Cornejo[1], Ignacio Arias[2], Alejandro Martínez[1,2], Mercedes Ibarra[2], Felipe Valencia[3]

1 Laboratory for Environmental Research in Arid Zones, LIMZA, Department of Mechanical Engineering, University of Tarapaca, Avda General Velásquez #1775, Arica, Chile

2 Fraunhofer Chile Research, Center for Solar Energy Technologies, Avda Vicuña Mackenna #4860, Santiago, Chile

3 Department of Electrical Engineering, University of Chile, Santiago, Chile

Abstract

In Chile, energy demand is projected around 34%, to the year 2030 respect of the actual demand. Which implies an increase in CO_2 emissions released into the atmosphere. Because of this, the Atacama desert presents itself as the main focus for the implementation of solar concentration technologies to satisfy the energetic solicitations of the country. For this reason, we focused to study, characterization and compare the surface of the solar field of three parabolic trough solar thermal power plants with nominal powers 30 MW, 50 MW and 100 MW with a solar multiple equal 1, in 16 locations of the Atacama desert. In addition, equipment was selected and established standard design conditions obtained the operational values of the most recognized plants in operation worldwide. For other hand, the solar resource of the Atacama desert was estimated using the Boland-Ridley-Lauret model (BRL), and as input data the global horizontal irradiation acquired of the solar explorer of the University of Chile, estimating the value of direct normal irradiation at the design point, the monthly and annual value for the 16 locations. In this way, the performance of two heat transfer fluids, such as, Therminol VP-1 and Syltherm 800 were analysed under the design conditions. As well as, the economic impact of these thermal oils in the solar field and LCOE were estimated. Similarly, full load operation hours, the annual electrical generation per location and its average per nominal power were estimated. As a consequence of this work, it is possible now to make a more accurate decision about the design of parabolic trough solar thermal power plants in the Atacama desert, proving to be an important contribution to make up for the lack practical/operational about this subject matter in Chile.

Keywords: Renewable Energy, Solar Energy, Solar Plant, Chile, Atacama desert, parabolic trough collector, heat transfer fluid

1. Introduction

The design of parabolic trough solar thermal power plants has received much attention in recent years due to their capabilities to provide clean energy to supply the nowadays growing demand of electricity. According to International Energy Agency (IEA), in 2017 the global demand of energy grew up 2.1% respect to the year 2010, which is equivalent to a rising of 14050 million of tons of petroleum equivalents (Mtoe) [1], and for 2035 such rising in petroleum equivalents is expected to be of 18608 Mtoe [2].

Due to the accelerated increase in the electric energy demand, the global warming, and the climate compromises established among the countries to reduce their own carbon footprint, parabolic trough solar thermal power plants have been investigated as a feasible alternative for dealing with the aforementioned requirements. However, it has been found that current methodologies available for the design of parabolic trough solar thermal power plants might lead to practical/operational issues, particularly in the Atacama Desert. Due to the solar resource of the Atacama Desert that registers an average daily global horizontal irradiation that exceeds 7,5 kWh/m^2 and 9 kWh/m^2 respect to the direct normal irradiance [3] and a surface of 105000 km^2, it becomes an appealing alternative to partially/totally supply the electric energy demand of Chile estimated in 97074 GWh by 2035 (an increase of 30.6% in the demand of electric energy with respect to the year 2020) [4].

doi:10.18086/swc.2019.08.02 Available at http://proceedings.ises.org

Worldwide, the methodologies used in the solar field design of plants depend on parameters such as geographical location, direct normal irradiance at the design point and the characteristics of the equipment selected, such as the aperture area of each solar collector assembly, solar receiver and the physical - chemical characteristics of the heat transfer fluid used, since, the latter determines the maximum permissible operating temperature of each loop. Typically, plants located in Europe and India, such as Andasol I, Extersol II, Manchasol I, Astexol II and Megha, have a typical configuration of 4 SCA/loop with a design radiation that varies from 800 W/m2 to 900 W/m^2 [5]. The methodologies used for the design of parabolic trough solar thermal power plants usually define an assembly of four solar collectors per loop, for plants designed for Europe or United States. Nevertheless, in the case of the Atacama Desert such a result cannot be directly applied, since, the use of Sylltherm 800 and Therminol VP-1 with four solar collectors per loop supplemented with the high indexes of solar irradiation in the Atacama desert drives the heat transfer fluids towards the loss of its thermal properties and its denaturation temperature.

The present paper presents a comparative analysis between the use of two heat transfer fluid in parabolic trough solar thermal power plants located at the Atacama Desert. In this comparative analysis, three and four solar collectors per loop are considered in both cases. But, for the Therminol VP-1 a pre heating stage was considered. Moreover, in the analysis 16 different locations in the Atacama Desert were considered. The solar resource was estimated, and three parabolic trough solar thermal power plants were assessed with nominal power 30 MW$_t$, 50 MW$_t$ and 100 MW$_t$. For comparison purposes, the economic impact in terms of the levelled cost of energy, the performance in terms of the full load operating hours, and the expected generation, were used as indicators. It is important to remark that, the analysis developed here considered parabolic trough solar thermal power plants without thermal energy storage. Thus, the present research is an important contribution to make up for the lack of practical/operational information regarding the design of parabolic trough solar thermal power plants under high indexes of solar irradiation in the Atacama desert, which could incentives the introduction of this technology for the high powered generation to National Electric System (SEN).

Nomenclature

D	Diffuse fraction	$f_{shading}$	Shading factor
DNI	Direct Normal Irradiance, W/m^2	$L_{Spacing}$	Spacing between loop
GHI	Global Horizontal Irradiance, W/m^2	W	Collector width, m
A_c	Aperture area of the solar collector	A	Area, m^2
E_d	Direct Normal Irradiance in the design point, W/m^2	$CO\&M$	Operating and maintenance costs
θ	Incident angle, °	CFR	Recuperation factor of capital
θ_z	Zenith Angle, °	C_{inv}	Cost of investment factor per kWh
δ	Declination angle, °	CF	Annual cost of fuel
ω	Hour angle, °	Ge	Annual electric generation
$k(\theta)$	Incidence angle modifier	CFR	Recuperation factor of capital
T_{amb}	Ambient Temperature	Kd	Discount rate
T_{out}	Heat Transfer Fluid output temperature	N	Horizon of the economic analysis
V_W	Wind speed, m/s	P_{br}	Gross electric power
$\dot{m}_{HTF}$	Mass flow rate of the heat transfer fluid, kg/s	***Abbreviations***	
$N°_{SCA/loop}$	Number of SCA per loop	CSP	Concentration Solar Power
ΔT_{loop}	Increasing temperature per loop	HTF	Heat Transfer Fluid
ΔT_{SCA}	Increasing temperature per SCA	FLH	Full Load operating Hours
$N°_{loop}$	Number of loops of the solar field	PTC	Parabolic Trough Collector
$C_p(T)$	Specific heat of water, kJ/kgK	$PTSTPP$	Parabolic Trough Solar Thermal Power Plant
$\dot{Q}_u$	Useful thermal power, W	SCA	Solar Collector Assembly
$\dot{Q}_s$	Useful radiant solar power, W	$LCOE$	Levelized Cost of Energy
$\dot{Q}_{losses}$	Thermal losses, W	TES	Thermal Energy Storage
		SGS	Steam Generation System

2. Parabolic Trough Solar Thermal Power Plant (PTSTPP)

The current section is devoted to explain what is a PTSTPP and how it works. Furthermore, the details included in the design of these power plants are introduced. Particular attention is paid in this section to the solar field, since it constitutes the main focus of this research. Nowadays, there are many CSP technologies, highlights the central tower, lineal Fresnel and parabolic trough collector. The last technology mentioned, leads the world market, because it is the technology with more development and maturity [6, 7], where Spain is the country with the largest number of this type of plants worldwide [8]. Indeed, PTC technology leads the world market of CSP, since, comprise around 85% of cumulative installed capacity [9]. Among the benefits of the parabolic trough collector technology are the abundant operational experience, a profitable and promising investment and the possibility to complement the solar resource with fossil fuels and other sources of renewable energy in uncomplicated ways [10].

The parabolic trough collector typical plant concentrates the DNI, using a series of parabolic mirrors that direct the beam of light to a receiver tube, where the HTF circulates [9]. The HTF more used on the industry are the thermal oils that limit the operation temperature of the solar field in lathe to 400°C. The lasts advance of the technology work are the molten salts, which allow a better efficiency of the plant. However, the molten salts must be over to 220°C due to avoid solidification [11].

PTSTPPs work through the Rankine cycle. Principally a field of PTCs and a power block composes them. Some PTSTPPs have auxiliary systems consisting on boilers of fossil fuels. Some of them have a TES, that generally utilises molten salts [12]. The power block has a SGS, condenser, feed-water heat exchangers and finally a steam turbine. Once the heat is collected by the HTF in the solar field, it is passed to the power block (Rankine cycle) through a series of heat exchanger. This power block is in charge of transforming the mechanic energy of the steam in electrical energy that is injected to the main grid [6].

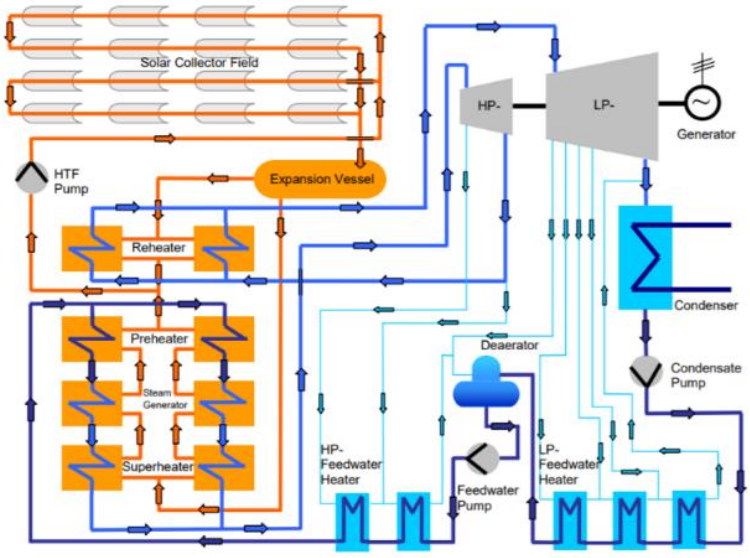

Figure 1. Diagram SEGS VI, United States [11]

2.1 Parabolic Trough Collector

The collector is a parabola shaped mirror in charge of capturing solar radiation and focusing it into the collector tube so that the solar radiation is converted in thermal energy. It is necessary to emphasize that how much collectors are placed on each assembly depends on the solar resource and the HTF used. A solar collector field is comprised by a series of solar PTCs, which automatically follow the sun position. Each collector is also known as SCA, and they are hydraulically connected first in series (loops) and then in parallel to other loops. To optimize the performance of the solar field and of this form avoids the optical losses of the system, its loops must be aligned North-South axis, following the sun East-West. These parameters are valid for systems that are in a latitude less than 46.06°, in the contrary case, each system of SCA must be aligned East-West axis [13]. Table 1 shows the principally parameters of the ET150, which is the parabolic trough collector selected in this research.

Table 1. Technical characteristics solar collector ET 150 [14]

Parameter	**ET150**	**Unit**
Focal Length	1.71	m
Absorber Radius	35	mm
Aperture Width	5.76	m
Aperture Area	828	m^2
Collector Length	148.5	m
Number of Modules per Drive	12	-
Number of Glass Facets	336	-
Number of Absorber Tubes	36	-
Mirror reflectivity	94	%
Weight of steel structure and pylons, per m^2 aperture area	18.5	kg

2.2 Receiver tube

The receiver is a tube located at the focus of the parabolic shaped mirrors. This tube allows that the HTF flow through it to capture the thermal energy provided by the solar radiation. Normally, the tube is designed with materials that maximise its absorbing covering properties, which indeed imply that the tube has special optical and thermal properties. These properties are important because the tube must support temperatures over the 400ºC. The second feature is of very high interest because, in the case of using molten salts as HTF, thermal losses might drive the salts towards their solidification state causing high impact damages in the infrastructure of the solar collector field. In this research we work with the receiver tube Schott PTR70, some typical values of the properties of this receiver tube are shown in Table 2 [15, 16].

Table 2. Technical Characteristics of the solar receiver Schott PTR70 [15]

Parameter		**Schott PTR70**	**Unit**
Dimension	Length (20°C)	4060	mm
Absorber	Outer diameter	70	mm
	Steel type	DIN 1.4541	
	Solar absorptance	$\alpha_{ISO} \geq 95.5$	%
		$\alpha_{ASTM} \geq 96$	%
	Thermal emittance	$\leq 9,5$	%
Glass envelope	Outer diameter	125	mm
	Solar transmittance	≥ 97	%
Thermal losses	A 400°C	< 250	W/m
	A 350°C	<165	W/m
	A 300°C	<110	W/m
	A 250°C	70	W/m
Operating pressure		≤ 41	Bar

2.3 Heat transfer fluid

The HTF is a fluid in charge of transforming the energy of the solar radiation into thermal energy. Often thermal oils, like Therminol VP-1 and Syltherm 800. The Therminol VP-1 is a synthetic heat transfer fluid, made by a eutectic mixture of 73.5% of diphenyl oxide ($C_{12}H_{10}O$) and 26.5% biphenyl ($C_{12}H_{10}$). It has a high evaporation temperature and was designed to satisfy the heat necessities of systems of high power of steam or liquid phases. This HTF combines an exceptional thermal stability and low viscosity properties. In fact, Therminol VP-1 has a low viscosity at its crystallization point (12°C) [12] and a maximum operational point of about 400°C (750F).

By contrast, the Syltherm 800 is a stable and durable fluid fabricated of silicone, which is based on dimethyl polysiloxane $(C_2H_6OSi)_n$ [12]. It was designed to work in liquid state when subject to high temperatures. The Syltherm 800 has a low crystallization point that preserves its thermal properties in a

range of temperatures of -40°C to 400°C (750°F). But, such range could be extended to 425°C, although this is not recommended. In comparison with the Therminol VP-1, the Syltherm 800 does not require a pre-heating stage, at locations with low environmental temperatures, to maintain its liquid state [17]. But, since it is more viscous than the Therminol VP-1, the convective heat transfer is lower affecting the heat transfer velocity from the radiation to the HTF. Consequently, the use of Syltherm 800 might require using more energy for its pumping [12], especially in the start-up of the plant. In spite of that fact, Syltherm 800 is a fluid that has a low pollution potential, is colourless and has a low oral toxicity, nevertheless, it is more expensive with a cost of 12 €/kg compared with the 4 €/kg of the Therminol VP-1. Table 3 presents a comparison of the main properties of the Syltherm 800 and the Therminol VP-1.

Table 3. Technical characteristics of heat transfer fluids [18, 19]

Properties	**Therminol VP-1**	**Syltherm 800**	
Composition	Biphenyl and Diphenyl Oxide	Dimethyl polysiloxane	
		As Supplied	After extended use
Appearance	Clear, water-white liquid	Clear yellow	Darkened
Flash point ASTM D92	124°C	160°C	≥ 35°C
Flash point ASTM D93	110°C	177°C	≥ 58°C
Autoignition point	621°C	385°C	385°C
Crystallizing point	12°C	-40°C	-40°C
Maximum film temperatura	430°C	427°C	427°C
Density (25°C)	1060 kg/m^3	936 kg/m^3	936 kg/m^3
Viscosity (25°C)	3.79 mPa*s	9.1 mPa*s	≥ 6 mPa*s
Specific Heat (25°C)	1.56 kJ/kgK	1.62 kJ/kgK	1.62 kJ/kgK
Specific Heat (300°C)	2.314 kJ/kgK	2.086 kJ/kgK	2.086 kJ/kgK

3. Design conditions

The particular features of the HTF used in the PTSTPP mainly determined these conditions. For example, to maximise the energy transfer from the solar radiation to the HTF, the heat transfer fluid must flow in a turbulent regimen throughout the receiver tube [20]. Such a regimen is obtained, in the case of Therminol VP-1, considering a Reynolds number of about $8x10^5$ and in the case of Syltherm 800, considering a Reynolds number of $4x10^5$. The difference between the two thermal oils arises from the fact that at the same operating conditions (temperature), the Syltherm 800 has a lesser density and dynamic viscosity than the Therminol VP-1. The main objective of this, is to maintain a flow mass fully developed and a velocity in the range of 0.5 m/s to 4 m/s [21]. Moreover, mass flow that circulates per each SCA must be in the order of 7.5 kg/s per loop, which are the optimal operating ranges for the Therminol VP-1 and the Syltherm 800 [7, 22]. Additionally, independent of the thermal oil used as HTF, the increasing temperature in each loop must be 100°C, where the input and output temperature must be around 293°C and 393°C respectively [5, 22]. It is important to point out that, currently worldwide PTSTPP already installed and designed with similar considerations can be found, such as, SEGS VI in United States with a nominal power of 30 MW, Agua Prieta ll in Mexico with a nominal power of 400 MW and Helioenergy 2 in Spain with a nominal power of 50 MW. All these power plants do not consider thermal energy storage systems, as the ones assessed in this paper.

The solar resource must be evaluated so that determinate the number of SCA per loop in the solar field. This must be made, ideally, at the exact location at which the plant will be placed. According to the international criterions, this value corresponding to the DNI at 12 o'clock (solar time) of the summer solstice in the southern hemisphere [23]. Furthermore, in this work no TES was considered, hence, the solar multiple will be 1, because no excess solar energy can be used for the power block. On another matter, the thermal performance of the Rankine cycle is considered as 38%, the steam generator efficiency 98% [5, 24] and the parasitic load consumption was established as 14% of the nominal power [25].

4. Methodology

The current investigation consisted in estimating the effect of high indexes of solar irradiation presents in the Atacama desert, in the design point in PTSTPPs that make use thermal oils as HTF, such as, Therminol VP-1 and Syltherm 800. For quantify the effects in the aperture area of the solar collector field, using ET150 and Schott PTR70. First, the solar resource must to be obtained and calculated for sixteen locations selected. Then, for each of those locations, the solar field was optimised. Finally, an economic analysis is realized. The Fig 2 shows the methodology used throughout this research.

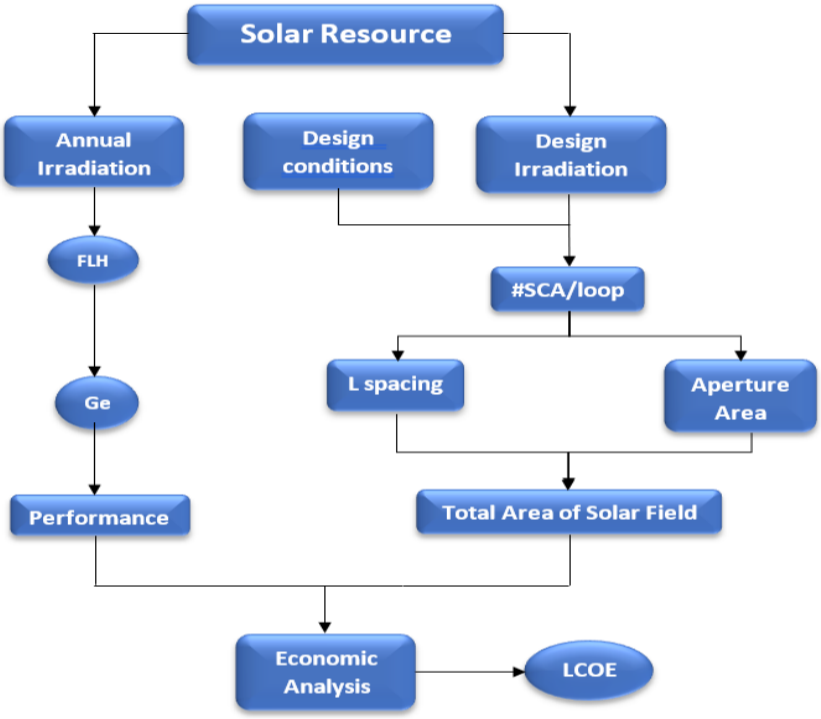

Figure 2. Methodology

Sixteen locations were selected over 1000 m above sea level along Atacama desert, so as to avoid to locate these places under the cloud layer. Due to above, the analysis is focused on the places that currently are more prone to become candidates for the implementation of parabolic trough solar thermal power plants. Table 4 shows the geographical coordinates of 16 locations selected.

Table 4. Geographical coordinates of selected locations

Location	Region	Latitude	Longitude	Altitude
1	XV	-18,754	-69,766	2107
2	XV	-18,774	-70,024	1243
3	XV	-18,132	-69,715	3760
4	XV	-19,464	-69,523	2146
5	I	-20,282	-69,284	2093
6	I	-20,456	-69,817	1142
7	I	-19,939	-69,298	2531
8	I	-20,604	-69,186	2238
9	II	-22,869	-69,140	2130
10	II	-23,633	-70,133	1034
11	II	-23,541	-68,225	2301
12	II	-24,640	-69,376	2247
13	III	-28,597	-70,402	2100
14	III	-27,235	-70,469	1006
15	III	-26,973	-69,769	2329
16	III	-27,764	-69,984	2091

4.1 Mathematical model for the characterization of the solar field

To obtain data of the solar irradiance, as well as other meteorological parameters of each location showed in the Table 4, the solar explorer of the University of Chile was used. For each location, the hourly profile was obtained in Typical Meteorological Year (TMY) format of GHI for the years 2004 to 2016. The estimation of the daily profile of fraction diffuse was done through the Boland-Ridley-Lauret model (BRL) [26]. The orientation of this type of plants depend its geographical location, where the cosine of the incident angle respect to the area of aperture of the solar collector depends of the rotation axis orientation. For plants oriented north-south with a tracking east-west [27], the cosine of incident angle is:

$$cos\theta = \sqrt{\cos^2(\theta_z) + \cos^2(\delta) * \sin^2(\omega)} \quad \text{(eq. 1)}$$

The incident solar energy over each parabolic trough in the design point was determined by Eq. (2). [28]. To determinate the useful power over each SCA, is very important determine the incident angle modifier, it was determined with Eq. (3), which is specific to Schott PTR 70 solar receiver. For other hand, because of that each location has different weather conditions, it is indispensable to estimate the thermal losses of the solar receiver of each SCA taking into consideration these parameters. So, the thermal losses of the solar collector selected in the design point can be determined by Eq. (4), suggested by NREL [16]. Additionally, useful power per SCA and the number of SCA per loop was modeled by Eq. (5) and Eq. (6).

$$\dot{Q}_s = A_c * E_d * \cos(\theta) \quad \text{(eq. 2)}$$

$$k(\theta) = 1 - 5{,}25097 * 10^{-4} * \left(\frac{\theta}{\cos(\theta)}\right) - 2{,}859621 * 10^{-5} * \left(\frac{\theta^2}{\cos(\theta)}\right) \quad \text{(eq. 3)}$$

$$\dot{Q}_{losses} = A_0 + A_1 * (T_{HTF} - T_{amb}) + A_2 * {T^2}_{HTF} + A_3 * {T^3}_{HTF} + A_4 * E_b * k(\theta) * {T^2}_{HTF} + \sqrt{V_W} * (A_5 + A_6 * (T_{HTF} - T_{amb})) \quad \text{(eq. 4)}$$

$$\dot{Q}_u = \dot{m}_{HTF} * \int_{T_{in}}^{T_{out}} C_p(T) * dT \quad \text{(eq. 5)}$$

$$N°_{SCA/loop} = \frac{\Delta T_{loop}}{\Delta T_{SCA}} \quad \text{(eq. 6)}$$

To determine the total extension of the solar field must be consider the separation between the loops that compose it. For that the shader factor per row of solar collectors must be defined by Eq. (7). Where, $f_{shading} \in [0,1]$. The value of $f_{shading} = 0$, represent that the solar collector is fully shaded, in contrast, if $f_{shading} = 1$ represent that the solar collector is not shaded. Of this form the total area of the solar collector field can be estimate with the Eq (8).

$$f_{shading} = \min\left[max\left[0, \frac{L_{Spacing}}{W} * \frac{cos(\theta_z)}{cos(\theta)}\right], 1\right] \quad \text{(eq. 7)}$$

$$A_T = A_{min} + L_{loop} * L_{Spacing} * \left(N°_{loop} - 1\right) \quad \text{(eq. 8)}$$

4.2 Economic analysis

The LCOE is the economic factor of the plants of electrical generation, because it reflects the minimum cost that the electricity must have for will be profitable. This economic indicator involves parameters as the G_e, CO&M, C_{inv}, CFR, as well as the annual costs associate to the use of fossil fuels. Of this form the LCOE was defined by Eq. (9) [29].

$$LCOE = \frac{CO\&M + CFR * C_{inv} + CF}{Ge} \quad \text{(eq. 9)}$$

Where the recuperation factor of the capital is expressed by Eq. (10) [30].

$$CFR = \frac{kd*(1+kd)^N}{(1+kd)^N-1} \quad \text{(eq. 10)}$$

For determine the annual electrical generation is necessary estimate the quantity of FLH. This parameter depends directly of the annual DNI value and the solar multiple, it was defined by Eq. (11) [31].

$$FLH = (2{,}5717 * DNI + 694) * (-0{,}0371 * SM^2 + 0{,}4171 * SM - 0{,}0744) \quad \text{(eq. 11)}$$

Of this mode the annual electricity generation is determine in function of the gross electric power injected on grid and the quantity of annual hours of operation to full load.

$$Ge = FLH * P_{br} \quad \text{(eq. 12)}$$

5. Discussion and Results

Of the equations underlying the calculation methodology of section 4, for each location that shows in the Table 4, The radiation in the design point was estimated, as well as other parameters involved to the design of solar field.

Table 5. Characterization per SCA of the solar field in the design point

Location	Desing radiation W/m^2	Annual DNI kWh/m^2	Tamb °C	V_w m/s	Cosθ	K(θ)	$\dot{Q}_s$ W	$\dot{Q}_{losses}$ W	$\dot{Q}_{useful}$ W
1	990	2.977	15	3.4	0.996	1	806683	34833	578874
2	947	2.925	15	3.4	0.996	1	772075	34758	552597
3	971	3.087	15	3.6	0.996	1	790839	34825	565843
4	976	2.984	15	3.3	0.996	1	795076	34793	569093
5	955	3.105	15	3.9	0.999	0.99609	779509	34801	549598
6	942	2.912	15	4.6	0.999	0.99386	769345	34861	540622
7	987	3.058	15	3.8	0.999	1	805476	34863	571751
8	975	3.153	15	3.6	0.999	0.99206	796366	34802	559817
9	1000	3.297	15	4.2	0.9999	0.99480	817483	34921	577149
10	1000	3.194	15	4.7	0.9999	0.99455	817481	34972	576945
11	1000	3.296	15	3.4	0.9999	0.99579	817489	34829	577856
12	1000	3.392	15	3.7	0.9999	0.99579	817489	34860	577826
13	1000	3.260	15	3.6	0.996	1	813931	34874	582027
14	961	2.834	15	3.8	0.998	1	784082	34821	560203
15	1000	3.392	15	3.6	0.998	1	815767	34868	582669
16	1000	3.301	15	3.9	0.998	1	815767	34907	582630

It is necessary to emphasize that, when the solar resource was evaluated, to each location showed in the Table 5 that presented DNI values in the design point over 1000 W/m^2, these values was normalized to 1000 W/m^2. This discernment was used because choose values of radiation of design over this value, means work most of the hours useful of sun with an auxiliary boiler of fuel fossil. As shown in Table 5, the estimate annual value of DNI of the locations selected is over 2000 kWh/m^2, this result attractive since an economic perspective. Also, the monthly values of DNI do not present differences substantial on the year, it favours the use of CSP technology. For other part, the annual daily average of DNI of all locations are between 7.5 kWh/m^2 and 10 kWh/m^2 [30]. Of the data shown in Table 5, through the Eq. (5) and Eq. (6) were determined the increasing temperature of each SCA and the number of SCA to obtain an increasing temperature of 100°C in each loop of the solar collector field. Obtaining the Fig. 3 and Fig 4. For other hand, the incidence angle modifier tends to 1 at the noon of the 21 December (summer solstice for the southern hemisphere), since, the zenith angle is in the highest point of the year. This phenomenon happens in places nearby to Ecuador as north of Chile.

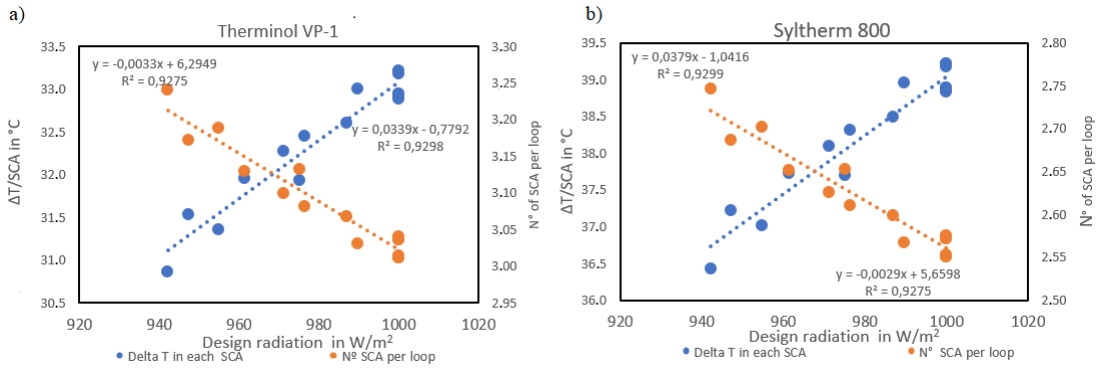

Figure 3. Comp$_a$rison between the design radiation, increasing temperature per SCA and number of SCA per loop

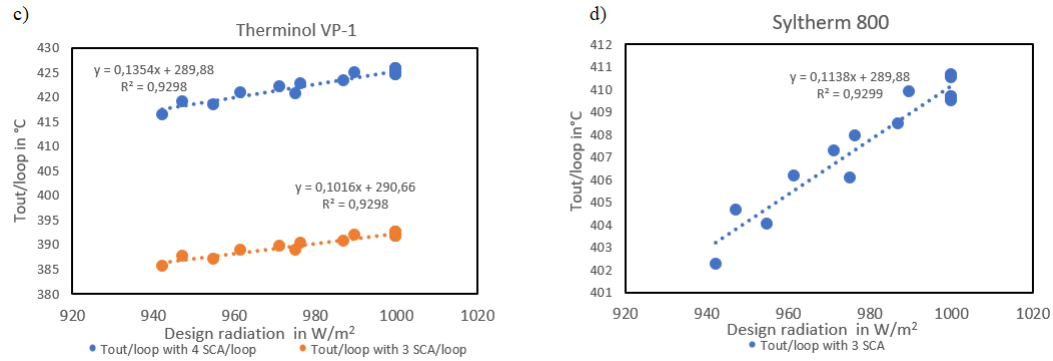

Figure 4. Comparison between the design radiation and outlet temperature of each loop

In Fig. 3 (a) and Fig. 3 (b) are possible observe that, if the design radiation increases, the output temperature in each SCA increasing, whereas the number of SCA per loop is reduced. This value is not an integer number and in the case of the thermal oil Therminol VP-1, is in the range of 3 SCA/loop – 3.25 SCA/loop. For other hand, for the thermal oil Syltherm 800 the value is in the range of 2.5 SCA/loop – 2.8 SCA/loop. However, the Fig. 4 (a) shows the effect on the output temperature of each loop for the thermal oil Therminol VP-1 when the number of SCA per loop is approximated to the top and bottom integer value. When this value is normalized to 4 SCA/loop is obtained output temperature over 400°C, which implies get out of focus large part of the solar collector field to prevent that the HTF works over its limit of operation temperature. Hence, the number of SCA per loop was normalized to 3 SCA/loop, obtaining output temperatures of each loop in the range of 386°C – 393°C. Whereas, the Fig. 4 (b) shows the effect on the output temperature of each loop for the Syltherm 800, in the case of this HTF was not necessary approximate to the bottom integer value. Since, the performance of each loop would not be optimum. Using Eq. (7) the shading hourly factor of each region was computed, obtaining the Fig. 5.

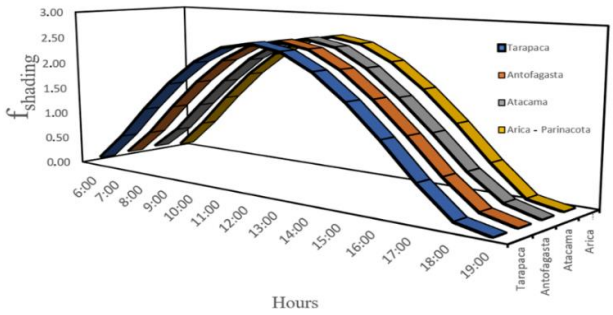

Figure 5. Hourly shading factor to different regions of the Atacama desert

According to results obtained, 15 meters of separation are enough to work more than 90% of useful hours of sun without shadow. Using this separation only 23% of the useful hours of sun will have partial shading. Due to above, between 07:30 hrs and 16:30 hrs there will not thermal losses respect to shading

between rows. Hence, using Eq. (8) the total area of the solar collector field was estimated for each nominal power and region.

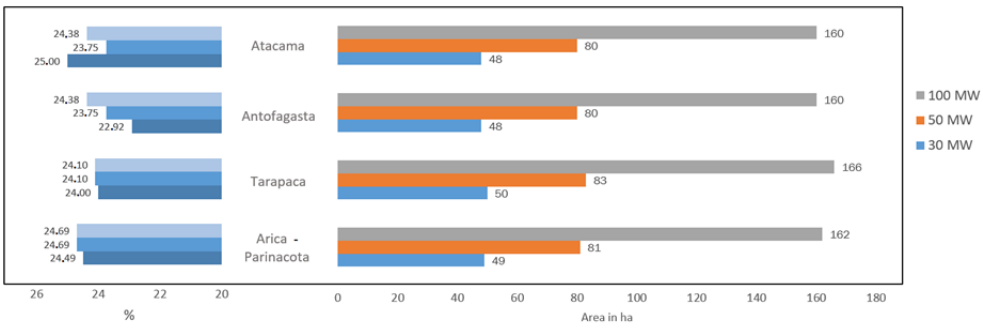

Figure 6. Percentage in the reduction of the solar collector field area using 3 SCA/loop instead of 4 SCA/loop

Fig. 6 shows the reduction percentage to use 3 SCA/loop instead of 4 SCA/loop. This reduction percentage is between 23% to 25% for all the nominal powers. Is necessary emphasize that, the Arica – Parinacota and Tarapaca regions were the places with most reduction percentual of solar collector field area, which on average is 24%. Of this mode, using equations underlying in the subsection 4.2, the average value of LCOE in USD/kWh of each parabolic trough solar thermal power plant was estimated. [32, 33].

Table 6. Parameters to analysis of LCOE

Parameter	**Value**	**Units**
Investment Cost SM=1		
Lower limit	4500	USD/kW
Upper limit	7150	USD/kW
Horizon analysis	30	Years
Discount rate	10	%
CFR	0.106	-
Percent of CO&M of Investment cost	1	%

Table 6 shows the main parameters to compute the LCOE for each PTSTPP. On the other hand, by incorporating the cost associated to use GNL to maintain out of the crystallization point to HTF Therminol VP-1 was not obtained a significative variation on the value of LCOE. Consequently, considering the economic factors of the inversion according to International Renewable Energy Agency (IRENA) [34] for parabolic trough solar thermal power plants without TES, the value of LCOE to each plant was computed and are in the range of 0.23 USD/kWh - 0.37 USD/kWh.

6. Conclusion

Solar radiation magnitude influences directly in the extension of the solar collector field, due to that, use 4 SCA/loop would be not recommendable, since the increasing temperature of each SCA would be more than the operational limit, being a deficient distribution. Consequently, use 3 SCA/loop would be recommendable, since this decision brings with it a reduction of aperture area of the solar collector field for each nominal power of 20% to 25%, however, the hypothetical use of 3 SCA/loop would makes it difficult the operation and maintenance of the plants. In the current market, there are only central configurations, with an even number of SCA/loop. Therefore, it is suggested to study the design of a PTC with less length than solar collector ET150 according to the climatic conditions of the Atacama desert.

Respect to the sixteen locations selected, 87% has values over 950W/m^2 of design radiation and only 12.5% has values in the range of 900 W/m^2 - 950 W/m^2 of design radiation. On average, the annual electrical generation of the PTSTPPs of 30 MW, 50 MW and 100 MW correspond to 77018 MWh, 128364 MWh and 256727 MWh respectively. Additionally, values of LCOE obtained are in the range to the international standard shown by IRENA, hence, the implementation of PTSTPPs in the Atacama desert is

economically viable. However, even though these technologies can compete with the conventional electrical generation in the energetic market, these are still in disadvantage with the conventional electrical generation whose LCOE is in the range of 0.05 USD/kWh to 0.17 USD/kWh depending of fossil fuel used.

Finally, we can conclude that is necessary approximately 1260, 756 and 378 plants of 30 MW, 50 MW and 100 MW respectively, to satisfy the energy demand forecast of Chile to the year 2030. Which means using around 612 km^2 to 617 km^2, representing approximately the 0.6% of the total extension of the Atacama desert using PTC. This research is expected to be a contribution to make an exponential leap in the use of this type of technology in the north of Chile.

7. Acknowledgments

The authors gratefully acknowledge the financial support of the Solar Energy Research Center, SERC Chile (CONICYT/FONDAP/15110019), as well as the Fraunhofer Chile Research with the project with basal code CSET 13CEI12-21803.

8. References

[1] International Energy Agency, Global Energy & CO_2 Status Report 2017, Paris, Francia, 2018.

[2] Z.M. Chen, G.Q. Chen, 2011. An overview of energy consumption of the globalized world economy. Energy Police. 39, pp. 5920-5928, https://doi.org/10.1016/j.enpol.2011.06.046.

[3] Rodrigo A. Escobar, Cristián Cortés, Alan Pino, Marcelo Salgado, Enio Bueno Pereira, Fernando Ramos Martins, John Boland, José Miguel Cardemil, 2015. Estimating the potential for solar energy utilization in Chile by satellite-derived data and ground station measurements. Solar Energy. 121, pp. 139-151, http://dx.doi.org/10.1016/j.solener.2015.08.034.

[4] Ministerio de Energía, Informe definitivo de previsión de demanda 2017-2037 Sistema Eléctrico Nacional y Sistemas Medianos, Comisión Nacional de Energía, Chile, 2017.

[5] M. J. Montes, A. Abándes, J.M. Martínez-Val, M. Valdés, 2009. Solar múltiple optimization for a solar-only thermal power plant, using oil as heat transfer fluid in the parabolic trough collectors. Solar Energy. 83, pp. 2165-2176, https://doi.org/10.1016/j.solener.2009.08.010.

[6] Xiaolei Li, Ershu Xu, Linrui Ma, Shuang Song, Li Xu, 2019. Modeling and dynamic simulation of a steam generation system for a parabolic trough solar power plant. Renewable Energy. 132, pp. 998-1017, https://doi.org/10.1016/j.renene.2018.06.094.

[7] Mario Biencinto, Rocío Bayón, Esther Rojas, Lourdes González, 2014. Simulation and assessment of operation strategies for solar thermal power plants with a thermocline storage tank. Solar Energy. 103, pp. 456-472, https://doi.org/10.1016/j.solener.2014.02.037.

[8] Electric Power Research Institute, Department of Energy, Renewable Energy Technology Characterizations, National Renewable Energy Laboratory, Topical Report, Washington D.C., United States, 1997.

[9] Roberto Leiva-Illanes, Rodrigo Escobar, José M. Cardemil, Diego-César Alarcón-Padilla, 2018. Comparison of the levelized cost and thermoeconomic methodologies – Cost allocation in a solar polygeneration plant to produce power, desalted water, cooling and process heat. Energy Conversion and Management. 168, pp. 215-229, https://doi.org/10.1016/j.enconman.2018.04.107.

[10] Wang Fuqiang, Cheng Ziming, Tan Jianyu, Yuan Yuan, Shuai Yong, Liu Linhua, 2017. Progress in concentrated solar power technology with parabolic trough collector system: A comprehensive review. Renewable and Sustainable Energy Reviews. 79, pp. 1314-1328, https://doi.org/10.1016/j.rser.2017.05.174.

[11] Evangelos Bellos, Christos Tzivanidis, Kimon A. Antonopoulos, 2017. A detailed working fluid investigation for solar parabolic trough collectors. Applied Thermal Engineering. 114, pp. 374-386, https://doi.org/10.1016/j.applthermaleng.2016.11.201.

[12] Gerard Preiró, Jaume Gasia, Laia Miró, Cristina Prieto, Luisa F. Cabeza, 2017. Influence of the heat transfer fluid in a CSP plant molten salts charging process. Renewable Energy. 113, pp. 148-158, http://dx.doi.org/10.1016/j.renene.2017.05.083.

[13] Y. Q. Song, Y. Xiang, Y. B. Liao, B. Zhang, L. Wu, H. T. Zhang, 2013. How to decide the alignment of the parabolic trough collector according to the local latitude, International Conference on Materials For Renewable Energy and Environment.

[14] Eckhard Lüpfert, Eduardo Zarza-Moya, Michael Geyer, Paul Nava, Josef Langenkamp, Wolfgang Schiel, Antonio Esteban, Rafael Osuna, Eli Mandelberg, 2003. Eurotrough Collector Qualification Complete - Performance Test Results from PSA, ISES Solar World Congress.

[15] Schott Solar, Schott PTR®70 Receivers, https://www.schott.com, 2019, accessed 20 febraury 2019.

[16] F. Burkholder, C. Kutscher, 2009. Heat Loss Testing of Schott's 2008 PTR70 Parabolic Trough Receiver. National Renewable Energy Laboratory. [NREL/TP-550-45633].

[17] C.P. McKay, E.I. Friedmann, B. Gómez-Silva, L. Cáceres-Villanueva, D.T. Andersen, R. Landheim, 2003. Temperature and moisture conditions for life in the extreme arid region of the Atacama Desert: four years of observations including the el niño of 1997-1998. Astrobiology. 3, pp. 393-406, https://doi.org/10.1089/153110703769016460.

[18] Dow, SYLTHERM™ 800 stabilized HTF, https://www.dow.com/en-us/product-search/sylthermsiliconefluids, 2019, accessed 21 febraury 2019.

[19] Solutia, Therminol VP-1, http://twt.mpei.ac.ru/tthb/hedh/htf-vp1.pdf, 2019, accessed 21 febraury 2019.

[20] Evangelos Bellos, Christos Tzivanidis, 2019. Alternative designs of parabolic trough solar collectors. Progress in Energy and Combustion Science. 71, pp. 81-117.

[21] Dongqiang Lei, Xuqiang Fu, Yucong Ren, FangyuanYao, Zhifeng Wang, 2019. Temperature and thermal stress analysis of parabolic trough receivers. Renewable Energy. 136, pp. 403-413, https://doi.org/10.1016/j.renene.2019.01.021.

[22] B. Zeroual, A. Moummi, 2012. Design of Parabolic Trough Collector Solar Field for Future Solar Thermal Power Plants in Algeria, Conference: Environment Friendly Energies and Applications (EFEA.

[23] E. Lüpfert, U. Hermann, H. Price, E. Zarza, R. Kistner, 2004. Towards standard performance analysis for parabolic trough collector fields, SolarPaces Conference, Mexico, Oaxaca.

[24] John A. Duffie, William A. Beckman, 2013. Solar Engineering of Thermal Processes, Fourth Edition, University of Wisconsin-Madison.

[25] Relebohile John Ramorakane, Frank Dinter, 2015. Evaluation of parasitic load consumption for a CSP plant, Stellenbosch University.

[26] Barbara Ridley, John Boland, P. Lauret, 2010. Modelling of diffuse solar fraction with multiple predictors. Renewable Energy. 35, pp. 478-483, https://doi.org/10.1016/j.renene.2009.07.018.

[27] Evangelos Bellos, Christos Tzivanidis, 2019. Alternative designs of parabolic trough solar collectors. Progress in Energy and Combustion Science. 71, pp. 81-117.

[28] Loreto Valenzuela, Rafael López-Martín, Eduardo Zarza, Optical and thermal performance of large-size parabolic-trough solar collectors from outdoor experiments: A test method and a case study, Energy, Volume 70, 2014, Pages 456-464, https://doi.org/10.1016/j.energy.2014.04.016.

[29] D. Kearney, Ulf Herrmann, P. Nava, B. Kelly, R. Mahoney, J. Pacheco, R. Cable, N. Potrovitza, D. Blake, H. Price, 2003. Assessment of a Molten Salt Heat Transfer Fluid in a Parabolic Trough Solar Field. Journal of Solar Energy Engineering. 125, pp. 170-176, https://doi.org/10.1115/1.1565087.

[30] Seif Eddine Trabelsi, Louy Qoaider, A. Guizani, 2018. Investigation of using molten salt as heat transfer fluid for dry cooled solar parabolic trough power plants under desert conditions. Energy Conversion and Management. 156, pp. 253-263, https://doi.org/10.1016/j.enconman.2017.10.101.

[31] Peter Viebahn, Yolanda Lechon, Franz Trieb, 2011. The potential role of concentrated solar power (CSP) in Africa and Europe—A dynamic assessment of technology development, cost development and life cycle inventories until 2050. Energy Police. 39, pp. 4420-4430.

[32] International Renewable Energy Agency, Renewable Energy Technologies: Cost Analysis Series, Volume 1: Power Sector, 2012, https://www.irena.org/publications, accessed 25 febraury 2019.

[33] Craig Turchi, Mark Mehos, Clifford K. Ho, Gregory J. Kolb, 2010. Current and Future costs for parabolic trough and Power Tower system in the US market, National Renewable Energy Laboratory, [NREL/CP-5500-49303].

[34] International Renewable Energy Agency, Renewable Power Generation Costs in 2017, IRENA, 2017. https://www.irena.org/publications, accessed 25 febraury 2019.